FEBS Letters

FEBS PRESS science publishing by scientists

RESEARCH ARTICLE

Two phosphoenolpyruvate carboxykinases with differing biochemical properties in *Chlamydomonas reinhardtii*

Florencia Torresi[1,2], Fernanda M. Rodriguez[2,3], Diego F. Gomez-Casati[1,2] and Mariana Martín[1,2]

1 Centro de Estudios Fotosintéticos y Bioquímicos (CEFOBI), Consejo Nacional de Investigaciones Científicas y Técnicas (CONICET), Rosario, Santa Fe, Argentina

2 Facultad de Ciencias Bioquímicas y Farmacéuticas, Universidad Nacional de Rosario, Santa Fe, Argentina

3 Instituto de Procesos Biotecnológicos y Químicos (IPROBYQ), Consejo Nacional de Investigaciones Científicas y Técnicas (CONICET), Rosario, Santa Fe, Argentina

Correspondence
M. Martín, CEFOBI-CONICET, Universidad Nacional de Rosario, Suipacha 531, S2002LRK Rosario, 2000 Rosario, Santa Fe, Argentina
Tel: +54 341 4371955
E-mail: martin@cefobi-conicet.gov.ar

(Received 29 November 2022, revised 13 January 2023, accepted 14 January 2023)

doi:10.1002/1873-3468.14590

Edited by Ulf-Ingo Flügge

Phosphoenolpyruvate carboxykinase (PEPCK) catalyses the reversible reaction of decarboxylation and phosphorylation of oxaloacetate (OAA) to generate phosphoenolpyruvate (PEP) and CO_2 playing mainly a gluconeogenic role in green algae. We found two PEPCK isoforms in *Chlamydomonas reinhardtii* and we cloned, purified and characterised both enzymes. *Chlre*PEPCK1 is more active as decarboxylase than *Chlre*PEPCK2. *Chlre*PEPCK1 is hexameric and its activity is affected by citrate, phenylalanine and malate, while *Chlre*PEPCK2 is monomeric and it is regulated by citrate, phenylalanine and glutamine. We postulate that the two PEPCK isoforms found originate from alternative splicing of the gene or regulated proteolysis of the enzyme. The presence of these two isoforms would be part of a mechanism to finely regulate the biological activity of PEPCKs.

Keywords: algal PEPCK; *Chlamydomonas reinhardtii*; PEPCK; phosphoenolpyruvate carboxykinase

Phosphoenolpyruvate carboxykinase (PEPCK) is an enzyme distributed in all groups of organisms [1]. It catalyses the reversible reaction of decarboxylation and phosphorylation of oxaloacetate (OAA) to generate phosphoenolpyruvate (PEP) and CO_2 [2], using a nucleotide or pyrophosphate (PPi) to transfer a phosphoryl group. Phosphoenolpyruvate carboxykinase requires two metal ions for activity *in vivo* (generally Mn^{2+} and Mg^{2+}). Based strictly on the phosphoryl donor substrate, three groups can be distinguished within the PEPCKs: the ATP-dependent PEPCKs, found in most alpha-, gamma- and epsilon proteobacteria and approximately half of delta proteobacteria, yeast, most fungi, algae, plants and trypanosomatids; the GTP (or ITP)-dependent PEPCKs, present in animals, insects and half of beta proteobacteria and delta proteobacteria and the fungus *Neocallimastix frontalis*; and the PPi-dependent PEPCKs found in a limited number of unicellular eukaryotes and bacteria, but not in archaea [3–5].

In the green lineage, PEPCK, as well as pyruvate, phosphate dikinase (PPDK) in some tissues of Angiosperms, is responsible for initiating gluconeogenesis. Phosphoenolpyruvate carboxykinase has a crucial role in plants during seed germination, channelling carbon released from lipids and proteins reserves to form sugars until the development of the photosynthetic apparatus [6–11]; in some C4 algae [12–16], and some C4 and CAM plants [17,18], it has a role in the photosynthetic assimilation of carbon, providing CO_2 for the Calvin cycle through the decarboxylation of the OAA derived from malate/aspartate and it has also been

Abbreviations
CAM, Crassulacean acid metabolism; OAA, oxaloacetate; PEP, phosphoenolpyruvate; PEPCK, phosphoenolpyruvate carboxykinase; TAP, Tris-acetate-phosphate; TCA, trichloroacetic acid.

suggested to be involved in nitrogen and amino acid metabolism [19,20]. The nature of the reaction that PEPCK catalyses, places this enzyme as an important link between the metabolism of organic acids, amino acids, lipids and sugars [20].

In recent years, green algae have been used as valuable resources with potential to address urgent industrial and agricultural demands. Particularly, *Chlamydomonas reinhardtii* became a model microalga of interest for pure and applied research due to the availability of genetic tools for its manipulation, the possibility of generating deficient mutants in different genes and because its genome is completely sequenced. However, despite the potential biotechnological uses of green algae and the numerous existing studies of PEPCK in Angiosperms, little is known about this enzyme in other photosynthetic organisms.

To better understand the function and biochemical properties of PEPCK in green algae, we analysed the presence of this protein in *C. reinhardtii* cells.Two possible PEPCK isoforms were identified. We further biochemically characterised the recombinant enzymes herein named *Chlre*PEPCK1 and *Chlre*PEPCK2. Both enzymes are functional *in vitro* showing different decarboxylating parameters, oligomerisation states and metabolites response.

The obtained results allow us to gain insight into the biochemical regulation of green algae PEPCK and to integrate this knowledge with the data available in the literature, to better understand PEPCK evolution and its role in central carbon metabolism.

Materials and methods

Database searches, sequence analysis and homology modelling

The primary structure of *Chlre*PEPCK1 was obtained from the Phytozome database [21] while the NCBI database (https://www.ncbi.nlm.nih.gov/protein/) was used to find *Chlre*PEPCK2 aminoacidic sequence. Subcellular localisation predictions were performed using PREDALGO program [22]. Multiple sequence alignment was carried out using CLUSTALW program [23]. Protein sequences included in the alignments were *Escherichia coli* PEPCK (p|A8A5L1.1), *Trypanosoma cruzi* PEPCK (1II2_A) and *Arabidopsis thaliana* PEPCKs (NP_195500.1 and NP_680468.1).

Culture conditions

Chlamydomonas reinhardtii cc1690 cells were grown either in liquid or on solid (supplemented with 1.5% (w/v) agar) Tris-acetate-phosphate (TAP) media [24] under cool fluorescent light at 150 μmol photons·m^{-2}·s^{-1} (12-h light/12-h dark cycles) at 24 °C. Liquid cultures were incubated on a rotary shaker.

Quantitative RT-PCR

Total RNA was extracted from *C. reinhardtii* cells using TRI reagent (Molecular Research Center, Inc, Cincinnati, OH, USA) according to the manufacturer's instructions. Quality of purified RNA was determined on 1.2% (w/v) agarose gel electrophoresis, and quantity determination on an EPOCH 2 Microplate Spectrophotometer (BioTek Instruments, Inc., Agilent Technologies, Inc, Santa Clara, CA, USA). The first-strand cDNAs were synthesised by M-MLV reverse transcriptase (Promega, Fitchburg, WI, USA) and an oligo-dT 18 primer. Primers used for qRT-PCR are listed in Table 1. EEF1 (eukaryotic translation elongation factor 1 alpha 2; CHLREDRAFT_132905) was used as an internal control, and the relative expression ratio was calculated as previously described [25]. The entire process of qRT-PCR was carried out with The StepOnePlus Real-Time PCR System (Applied Biosystems, Foster City, CA, USA) under the following conditions: 2-min denaturation at 94 °C; 40 cycles at 94 °C for 10 s, 60 °C for 15 s and 72 °C for 20 s, followed by 10 min extension at 72 °C. Three replicates were performed for each sample. Melt curve analysis was conducted to confirm the specificity of each assay.

Table 1. Oligonucleotide primers.

Primer	Sequence (5′–> 3′)	Use
CrPEPCK UP	AAACATATGGCTCCCGTCGTCAAG	Cloning *Chlre*PEPCK1 from *C. reinhardtii* cDNA
CrPEPCK DW	ATTCTCGAGTTACTGCGTCTTGAAG	Cloning *Chlre*PEPCKs from *C. reinhardtii* cDNA
CrPEPCK2 UP	AAACATATGATGCAGTTCGTCCTG	Cloning *Chlre*PEPCK2 from *C. reinhardtii* cDNA
qPCK1 UP	CGCCATGCGGTTCACCAACA	qRT-PCR *Chlre*PEPCK1
qPCK1 DW	GCCATCTCGTACAGCTGGGGG	qRT-PCR *Chlre*PEPCK1
qPCK2 UP	CTGTCGGCGGATCCCAAGC	qRT-PCR *Chlre*PEPCKs
qPCK2 DW	CACGTTCTCCAGAACCGTG	qRT-PCR *Chlre*PEPCKs
EEF1 UP	CTAGGATGCTAACCGCGCAAGAG	qRT-PCR internal control *EEF1*
EEF1 DW	AACAGCGAAGCTCCACGCAC	qRT-PCR internal control *EEF1*

Statistical differences among the data were determined using GRAPHPAD PRISM (GraphPad Software Inc, San Diego, CA, USA).

Immunoblot analysis

For immunoblot analysis, proteins were extracted from *C. reinhardtii* cells using two different protocols. One of them includes a step of cells lysis with TRI reagent (Molecular Research Center, Inc) which combines phenol and guanidine thiocyanate in a mono-phase solution; a protein precipitation step with acetone; three wash steps with 0.3 M guanidine hydrochloride in 95% (v/v) ethanol + 2.5% (v/v) glycerol and the final protein solubilisation step with 10 M urea. This extraction protocol has been adopted in our laboratory as an efficient method for obtaining protein extracts from algae [26,27]. The second extraction method includes a extraction, precipitation and denaturation step with 100% (v/v) cold trichloroacetic acid (TCA); three consecutive rinsing steps with 5% (v/v) TCA, ethanol and 90% (v/v) acetone and the solubilisation step in SDS/PAGE loading buffer [28,29].

SDS/PAGE was performed on 10% (w/v) bis-acrylamide gels. The gels were subsequently blotted to a 0.45 μm nitrocellulose membrane (Amersham Biosciences, Amersham, UK) at a constant current of 100 mA for 1 h at 4 °C. The membranes were first blocked with 5% (w/v) low-fat milk in TBS at room temperature for 2 h, washed three times with TBS for 10 min and then probed with the antibody of interest (i.e. an a-6-His antibody (Santa Cruz Biotechnology Inc, Dallas, TX, USA)) or polyclonal antibodies raised against recombinant *Ananas comosus* PEPCK [30] affinity-purified against *Chlre*PEPCK as described by Plaxton [31]. After three 10-min washes with TBST (Tris-buffered saline with 0.1% Tween® 20 (v/v) detergent), the membranes were incubated with a Goat a-rabbit IgG, Horseradish Peroxidase (HRP) conjugated for 1 h at room temperature, followed by three 10-min washes with TBST. Chemiluminescent detection was performed with Biolumina detection reagent (Kalium Technologies, Bernal, Argentina).

Molecular cloning, expression and purification of *Chlre*PEPCKs

Using cDNA as template, the open reading frame (ORF) coding for the mature *Chlre*PEPCK1 (lacking the first 24 amino acid residues of the predicted chloroplast transit peptide) was amplified using oligonucleotides CrPEPCK-UP and CrPEPCK-DW (Table 1, restriction sites underlined) and cloned into pGEM-T Easy vector system (Promega) for subsequent subclonation into the NdeI and XhoI sites of pET28-a expression vector. *Chlre*PEPCK1 sequence was confirmed by DNA sequencing (Macrogen Inc., Seoul, Republic of Korea). The resulting plasmid pFtor1 (pET28a/ChlrePEPCK1) was used as a template to obtain the ORF coding for *Chlre*PEPCK2 with the primers CrPEPCK2 UP and CrPEPCK-DW (Table 1, restriction sites underlined) and it was also cloned into the NdeI and XhoI sites of pET28-a to obtain the plasmid pFtor2 (pET28a/ChlrePEPCK2). We transformed *E. coli* BL21 (DE3) pLysS cells with pFtor1 or pFtor2. Cells expressing the His-tagged recombinant proteins were grown overnight at 37 °C with shaking in Luria-Bertani (LB) medium supplemented with 50 $\mu g \cdot mL^{-1}$ chloramphenicol and 30 $\mu g \cdot mL^{-1}$ kanamycin. The overnight cultures were inoculated (1 : 100) into 400 mL of fresh LB medium until the optical density at 600 nm reached 0.4–0.6 and protein expression was induced by the addition of 0.5 mM isopropyl β-D-1-thiogalactopyranoside (IPTG). After 3 h at 37 °C for cells expressing *Chlre*PEPCK1 and 4 h at 28 °C for those expressing *Chlre*PEPCK2, cells were harvested and resuspended in lysis buffer (100 mM Tris–HCl pH 8.5, 5 mM $MgCl_2$, 2 mM EDTA, 20% (v/v) glycerol, 1 mM phenylmethylsulfonyl fluoride (PMSF) and 1 mM dithiothreitol (DTT)) and disrupted by sonication. Cell debris was separated by centrifugation at 12 000 ***g*** for 20 min at 4 °C, and the supernatant was recovered. Protein purification was performed with standard Ni^{+2} affinity chromatography using Ni-NTA agarose resin (MCLAB). Amicon® Ultra 15 mL filters were used for protein desalting and concentration. To determine protein concentration, purified samples were loaded into 10% (w/v) polyacrylamide gels together with bovine serum albumin (BSA) standards ranging in quantities of 0.1–2 μg. Gels were stained with Coomassie Brilliant Blue and densitometry of protein bands was measured with Gel-Pro Analyzer (v. 4.0, Media Cybernetics Inc., Bethesda, MD, USA). The concentrated protein was stored at −80 °C with the addition of 15% (v/v) glycerol until use.

Gel filtration

The apparent molecular mass of the *Chlre*PEPCK1 and *Chlre*PEPCK2 proteins was investigated by size exclusion column chromatography (Superdex 200 10/300 GL; GE Healthcare, Uppsala, Sweden). The column was equilibrated and performed at 0.2 $mL \cdot min^{-1}$ with buffer: 100 mM Tris pH 8.5, 2 mM EDTA, 5 mM $MgCl_2$, 10% v/v glycerol, 1 mM PMSF, and 1 mM DTT. The column was calibrated with the following standards: ferritin (443 kDa), catalase (240 kDa), human serum albumin (67 kDa), ovoalbumin (45 kDa) and chymotrypsin (25 kDa). The partition coefficient (K_{av}) was determined by the formula $K_{av} = (V_e - V_o)/(V_t - V_o)$, where V_e is the elution volume, V_o the void volume and V_t is the total volume of the column. The apparent molecular mass was determined from plot of partition coefficient as function of the logarithm of molecular mass.

Assays of activity and kinetic studies

*Chlre*PEPCKs activities were determined spectrophotometrically by following NADH oxidation at 340 nm. One unit of enzyme activity (U) is defined as the amount of enzyme resulting in the consumption of 1 μmol of NADH per minute. Assay conditions described previously in the literature [8,30] were optimised to ensure that maximum PEPCK activity was measured. The *Chlre*PEPCK carboxylation reaction mixture contained 100 mM Bis-Tris, pH 6.0, 50 mM $NaHCO_3$, 4 mM PEP, 0.15 mM NADH, 0.2 mM ADP, 2 mM $MgCl_2$, 1 mM $MnCl_2$ and 10 units malate dehydrogenase. The PEPCK decarboxylation reaction was assayed in a medium containing 100 mM Hepes-NaOH, pH 7.0, 0.5 mM OAA, 2 mM $MgCl_2$, 1 mM $MnCl_2$, 2 mM ATP, 0.4 mM ADP, 0.15 mM NADH, 5 units lactate dehydrogenase (LDH) and 2 units pyruvate kinase (PK). The OAA was prepared just before use and PEPCK activities were corrected for nonenzymatic OAA breakdown. The assays were performed in 200 μL at 25 °C. For the pH- and temperature-dependence studies, substrate and cofactor concentrations were saturating in the entire pH (5.5–8.5) and temperature (10–35 °C) range tested. Changes in absorbance were linear during the assayed time, and the activity was proportional to the amount of enzyme used. Activity values informed are the average of at least three independent measurements.

Results and discussion

PEPCK expression analysis in *C. reinhardtii* cells

Chlamydomonas reinhardtii genome has a locus (Cre02.g141400) coding for a putative PEPCK protein (*Chlre*PEPCK) [21]. The *Chlre*PEPCK polypeptide sequence was aligned with the sequences of PEPCKs from *Escherichia coli* (*Ec*PEPCK), *Trypanosoma cuzi* (*TcrPEPCK*) and *Arabidopsis thaliana* (*Ath*PEPCK1 and *Ath*PEPCK2; Fig. 1). A high degree of conservation can be observed in the different domains described as essential for PEPCK activity and substrate binding: PEPCK domain, kinase 1a and kinase 2 domains and ATP binding motif (yellow, blue, light blue and orange boxes, Fig. 1) [32,33]. Apart from those domains, all proteins share residues that are part of the active site: G110, R111, H263, L300, Y329, A330, K331, E340, I343, N375, R377, T431, F456 and R503 (*Chlre*PEPCK numbering; green boxes, Fig. 1). A marked difference can be noticed in the N-terminus: *Ath*PEPCKs have a regulatory region of 12–15 kDa that is absent in *Chlre*PEPCK. This region, present in all vascular PEPCKs, contains phosphorylation sites and is affected by proteolysis during the biochemical extraction of plant tissues [34–39].

Thus, the *Chlre*PEPCK can be classified as an ATP-dependent PEPCK and its amino acid sequence contains all catalytic and substrate binding domains required for PEPCK activity but lacks the regulatory N-terminal sequence characteristic of plant PEPCKs.

The presence of PEPCK protein was analysed on *C. reinhardtii* extracts in the exponential growth phase (OD_{750} close to 2) by western blot using a-PEPCK antibodies. Two immunoreactive bands of PEPCK were found: one of 68 and the other of 62 kDa (Fig. 2A). The possibility of unspecific proteolysis during the preparation of extracts was discarded because the isolation of proteins was performed under highly denaturing conditions with TRI reagent or TCA (see Materials and methods section) so that the proteases are inactive during both procedures. Thus, while we only found a single gene that codes for PEPCK in *Chlamydomonas* (Cre02.g141400), these experiments show the presence of two isoforms of the enzyme in the green alga. PEPCK isoforms of different molecular mass has been previously reported for *A. comosus* [30], *Zea mays* [36] and *A. thaliana* leaves [40].

These two isoforms could be the product of post-translational modification *in vivo* by specific proteases or alternative splicing of *PEPCK* transcript. *Ath*-PEPCK1 has been identified as a substrate of *A. thaliana* metacaspase-9 [41]. Metacaspases are present in *Chlamydomonas* [42] and the position of the recognition sequence in *Chlre*PEPCK primary structure (Fig. 1, pink line) would give a protein with an apparent molecular mass similar to that of the lower protein band observed in the a-PEPCK immunoblot.

Concerning the second possibility, it is reported that around 20% of *Chlamydomonas* genes show alternative splicing [43] and according to the NCBI database, the presence of a splice variant of PEPCK (XP_001694963.1) of 557 amino acidic residues was affirmed until August 2021 when that record was removed as a result of standard genome annotation processing. This variant lacks 55 amino acids at the N terminus which might include a chloroplast transit peptide of 24 residues according to PredAlgo program. Thus, according to *in silico* predictions, the heaviest *Chlre*PEPCK (herein called *Chlre*PEPCK1) would be a chloroplastic protein while the lightest (*Chlre*PEPCK2) would be located in the cytosol.

The transcriptional expression was studied performing RT-qPCR with specific primers (Table 1). Two pairs of primers were used: a pair that hybridises in the middle of the transcript *PEPCK* and a pair that hybridises only in the 5′ region of *PEPCK* (Fig. 2B, Table 1). The first pair would detect both transcripts: *ChlrePEPCK1* and *ChlrePEPCK2*, while the second

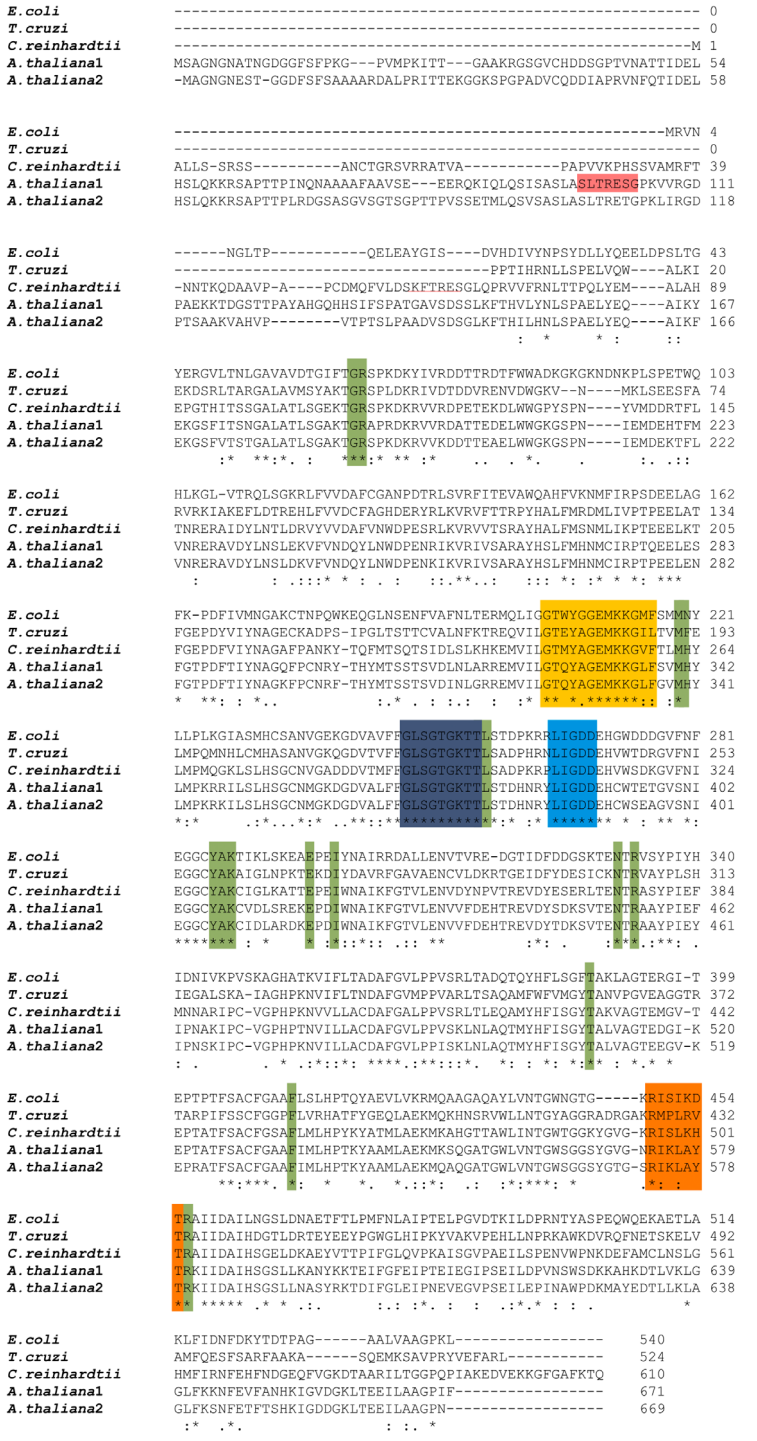

Fig. 1. Amino acidic sequences alignment of PEPCKs. Amino acidic sequence alignment of *C. reinhardtii* putative PEPCK with the PEPCK from *E. coli*, *T. cruzi* and *A. thaliana*. The yellow box highlights the PCK-specific domain which is conserved in all PEPCKs aligned. The blue box shows the Kinase-1a sequence, or P-loop motif, which interacts with the phosphoryl oxygen atoms of ATP and is perfectly conserved in these PEPCKs. The light blue box indicates the Kinase 2 sequence, which binds the Mg cation and is also conserved in all PEPCKs. The ATP-binding motif is shown in the orange box. Other conserved residues for the substrate union or PEPCK catalysis are highlighted in green. The pink box shows the metacaspase-9 recognition site of *A. thaliana* PEPCK1.

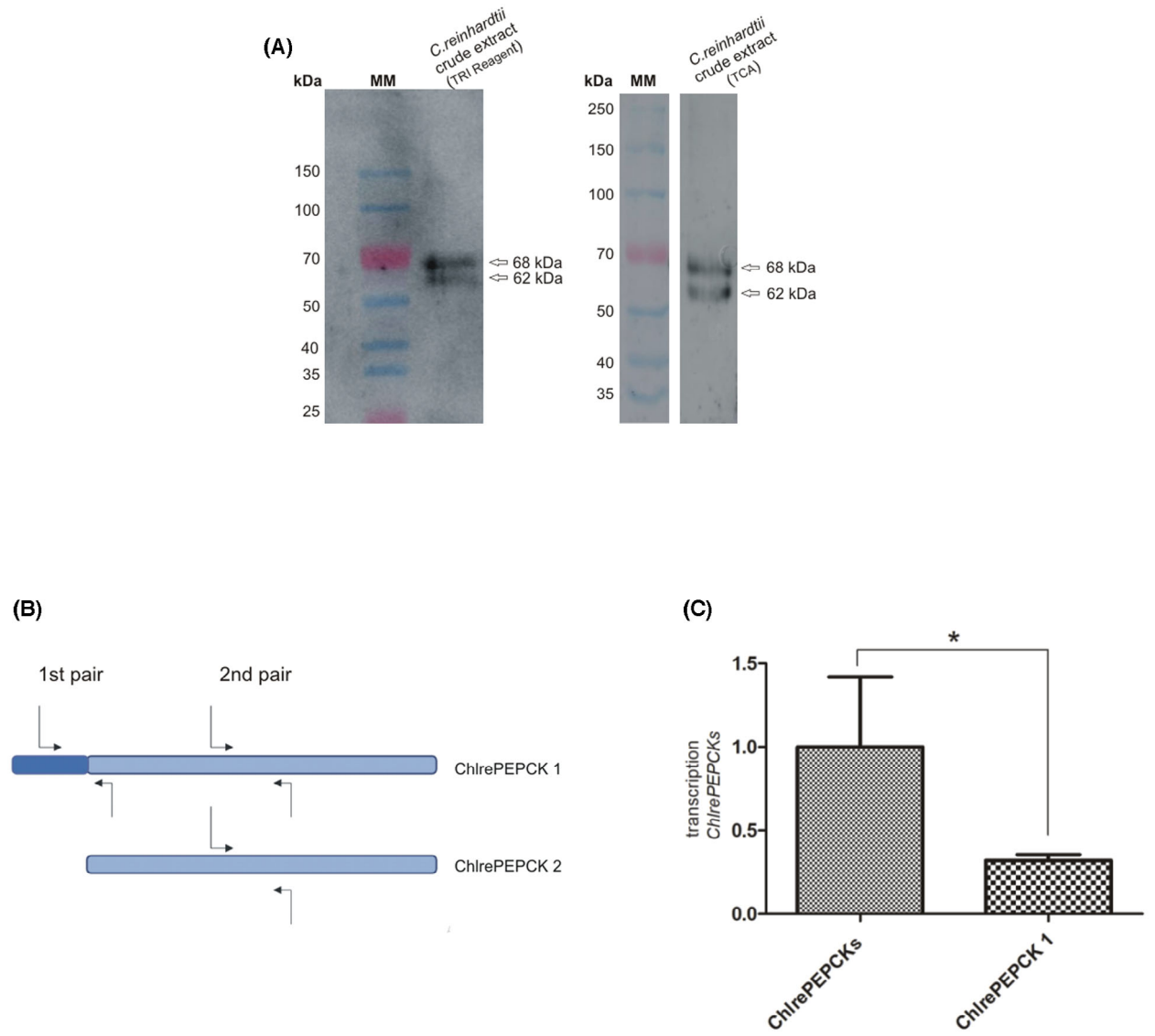

Fig. 2. PEPCK protein expression in *C. reinhardtii* cells. (A) SDS/PAGE of *C. reinhardtii* cells crude extracts analysed by western blotting. For SDS/PAGE, *C. reinhardtii* total protein extract obtained with TRI reagent or TCA were loaded. a-PEPCK: a-PEPCK antibody immunopurified for *Chlre*PEPCK1 protein. MM, molecular mass. Numbers indicate the molecular masses of markers in kDa. Tri-color Prestained Protein Ladder (GenBiotech, Caba, Argentina) was used. (B) Schematic representation of primers hybridisation in the PEPCKs putative transcripts. (C) Quantitative RT-PCR analysis of *PEPCK* transcripts levels in cells of *C. reinhardtii*. *EEF1*was used as an internal control. Relative expression for PEPCKs ($2^{-\Delta Ct}$) was considered, to normalise and simplify data. The other value was obtained by dividing it to the original value from *PEPCKs*. Bars represent the means ± SEM of three independent experiments. The asterisk indicates a statistical difference ($P < 0.05$) between relative gene expressions (*t*-test).

pair would only detect the *ChlrePEPCK1*. The expression found using the second pair of primers (only *ChlrePEPCK1* transcripts detected) was threefold lower than that found using the first pair (Fig. 2C). These results indicate that two transcripts *PEPCK* exist in *C. reinhardtii* and that one of them lacks the 5′ region, as described in the removed NCBI data.

Recombinant expression and purification of the *Chlre*PEPCKs

In order to characterise *Chlre*PEPCK1 and *Chlre*-PEPCK2, the gene molecular cloning, expression and production of the recombinant proteins were carried out (see Materials and methods section).

*Chlre*PEPCK1 and *Chlre*PEPCK2 were expressed in *E. coli* BL21 pLysS strain at 37 and 28 °C, respectively, and purified to homogeneity by Ni^{2+} affinity chromatography. The His6-tagged proteins *Chlre*PEPCK1 and *Chlre*PEPCK2 showed molecular masses of about 68 and 62 kDa and produce single bands on SDS/PAGE (Fig. 3A), which were confirmed by western blot analysis using a-His antibodies and affinity-purified a-PEPCK antibodies (Fig. 3B).

Kinetic properties of *Chlre*PEPCKs

As previously described for other PEPCKs, *Chlre*PEPCKs activity is strictly dependent on the presence of Mn^{2+} in the assay medium. *Chlre*PEPCKs also require the presence of a thiol-reducing compound in the assay medium for maximum activity; 4 mM 2-Mercaptoethanol increases the activity about 40%.

Both *Chlre*PEPCKs showed the maximal activities in a range between 15 and 25 °C (data not shown). In reference to pH dependence, they have also a similar pattern showing the OAA decarboxylating reaction the strongest pH dependence in both recombinant enzymes. The maximum velocity was assayed at pH 7 for decarboxylation and at pH 6 for PEP carboxylation (Fig. 4A).

Then, the kinetic parameters for the carboxylation and decarboxylation reactions for the recombinant enzymes were determined at pH 6 and 7, respectively, and at 25 °C. The saturation curves obtained when the rates of the reactions were analysed as a function of OAA, ATP, PEP and ADP concentrations in the presence of saturating concentrations of co-substrates were all hyperbolic (Fig. 4B,C).

For the carboxylation reaction, no significant differences were found in the values of K_m or V_{max} between *Chlre*PEPCK1 and *Chlre*PEPCK2 (Fig. 4B). K_m values for the *Chlre*PEPCK1 were 0.56 ± 0.04 mM for PEP and 0.10 ± 0.01 mM for ADP and for the *Chlre*PEPCK2 0.67 ± 0.08 mM for PEP and 0.17 ± 0.03 mM for ADP. The V_{max} of carboxylation of PEP was of 6.0 ± 0.2 $U{\cdot}mg^{-1}$ for *Chlre*PEPCK1 and of 6.1 ± 0.3 U mg^{-1} for *Chlre*PEPCK2 (Fig. 4B).

However, for the decarboxylation reaction, the *Chlre*PEPCK1 showed a higher value of V_{max} (9.6 ± 0.3 vs. 4.9 ± 0.3 $U{\cdot}mg^{-1}$ of the *Chlre*PEPCK2; Fig. 4C) and the values of K_m were also different: K_m values for the *Chlre*PEPCK1 were 67 ± 8 μM for OAA and 85 ± 9 μM for ATP and for the *Chlre*PEPCK2, the K_m was of 28 ± 9 μM for OAA and 37 ± 6 μM for ATP. These results suggest that the lack of those 55 amino acid residues in the N-ter *Chlre*PEPCK2 affects the enzyme decarboxylating properties, improving its affinity for the substrates OAA and ATP but decreasing the V_{max}.

We compared maximal activities of *Chlre*PEPCKs with those from C3, C4 and CAM plants PEPCKs and found that *Chlre*PEPCKs are less active than the PEPCKs of the C3 plant *Cucumis sativus* (41 and 48 $U{\cdot}mg^{-1}$) [37,44]; the C4 plants *Panicum maximum* (41.6 $U{\cdot}mg^{-1}$) [45], *Chloris gayana* (36 $U{\cdot}mg^{-1}$) [46] and *Urochloa panicoides* (42 $U{\cdot}mg^{-1}$) [46] and the CAM plant *A. comosus* (17 $U{\cdot}mg^{-1}$) [30]. However, *Chlre*PEPCKs are more active than the C3 *A. thaliana*

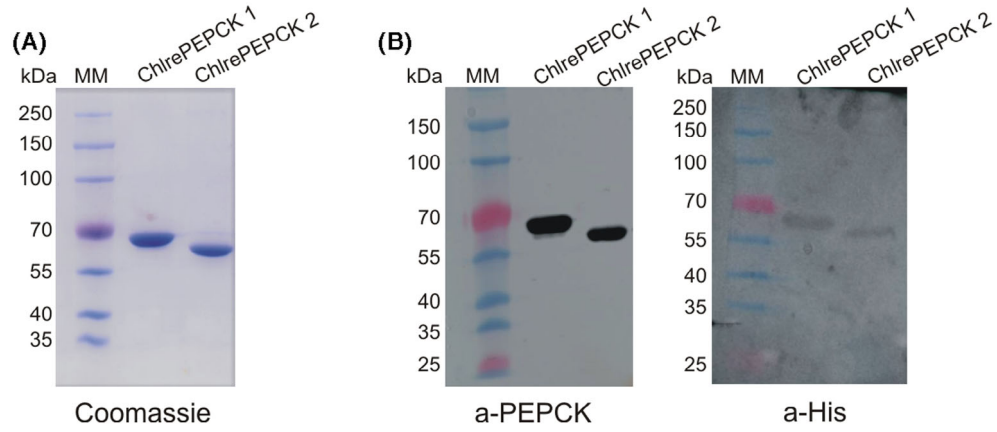

Fig. 3. Electrophoretic analysis of recombinant *Chlre*PEPCKs. (A) Coomassie blue staining of an SDS/PAGE of purified *Chlre*PEPCK1 and *Chlre*PEPCK2. (B) SDS/PAGE of *Chlre*PEPCKs analysed by western blotting. a-His, anti-His antibody; a-PEPCK, anti-PEPCK antibody immunopurified for *Chlre*PEPCK1 protein. For SDS/PAGE 2.5 μg of *Chlre*PEPCKs was loaded. MM, molecular mass (Tri-color Pre-stained Protein Ladder, GenBiotech). Numbers indicate the molecular masses of markers in kDa.

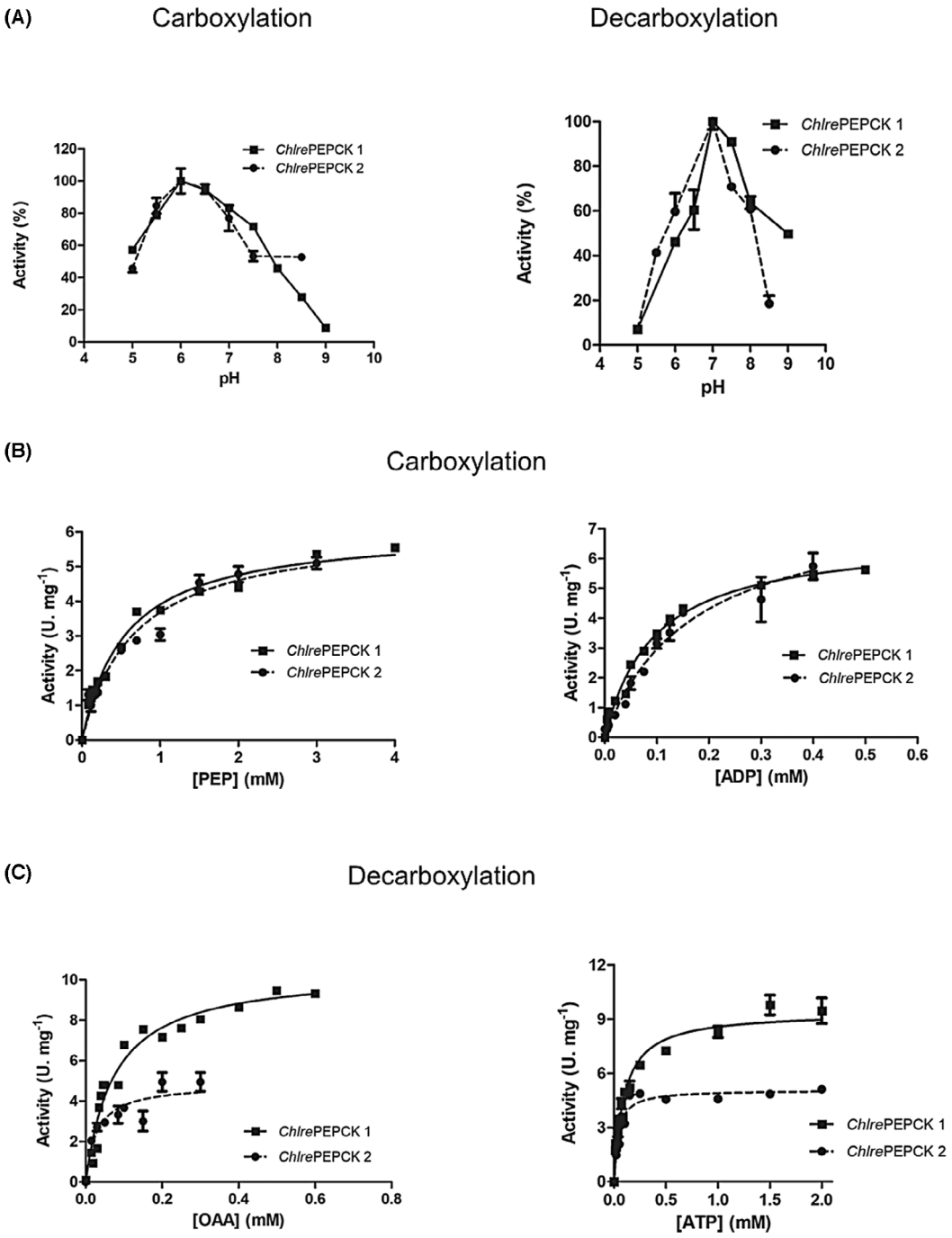

Fig. 4. Kinetic characterisation of *Chlre*PEPCKs. (A) Effect of pH on the activity of recombinant *Chlre*PEPCKs. Dependence of *Chlre*PEPCKs activity on pH was assayed in the carboxylating or decarboxylating direction using 26 mM imidazole; 4 mM Hepes; 40 mM Tris as buffer. Buffer pH values were adjusted to the values shown in the graphic and used to assay the enzyme. *Chlre*PEPCK1 activity is indicated by squares and continuous line. *Chlre*PEPCK2 activity is indicated by circles and dashed line. (B) PEP and ADP dependence of *Chlre*PEPCKs carboxylation activity. Each curve was made using the variable substrate concentration described in the figure and a fixed substrate concentration of 0.5 mM ADP or 4 mM PEP. Each point represents the mean ± SEM of three independent data sets. *Chlre*PEPCK1 activity is indicated by squares and continuous line. *Chlre*PEPCK2 activity is indicated by circles and dashed line. (C) OAA and ATP dependence of *Chlre*PEPCKs decarboxylation activity. Each curve was made using the variable substrate concentration described in the figure and a fixed substrate concentration of 2 mM ATP or 0.5 mM OAA. Each point represents the mean ± SEM of three independent data sets. *Chlre*PEPCK1 activity is indicated by squares and continuous line. *Chlre*PEPCK2 activity is indicated by circles and dashed line.

*Ath*PEPCK1 (2.6 U·mg^{-1}) [40] and similar to *Ath*-PEPCK2 (5.4 U·mg^{-1}) [40].

Modulation of *Chlre*PEPCKs activities by metabolites

The partitioning of carbon skeletons between PEP and OAA by the action of PEPCK is potentially important in the inter-conversion of sugars, organic acids, amino acids, aromatic compounds and lipids. That is why the enzyme must be strictly regulated [39].

To survey potential regulatory mechanisms of algae PEPCKs, the response of the purified enzymes to several metabolites, including glycolytic and Krebs cycle intermediates and amino acids, was tested *Chlre*-PEPCK1 and *Chlre*PEPCK2 show different susceptibility to some metabolites *in vitro*. No significant effects were observed with glucose 1-phosphate, fructose 1,6-BP, succinate, alanine, arginine and glycine in the *Chlre*PEPCKs reactions. However, we found that carboxylation by *Chlre*PEPCK1 (Fig. 5A) and *Chlre*PEPCK2 (Fig. 5B) was inhibited by citrate (23% inhibition) and phenylalanine (30% inhibition) when we used 2 mM of each metabolite in the reaction. *Chlre*PEPCK2 carboxylation was also affected by glutamine (42% inhibition; Fig. 5B). Decarboxylation by *Chlre*PEPCK1 is activated by phenylalanine and malate (2 mM; about 1.5 and 1.3-fold, respectively; Fig. 5C). By contrast, *Chlre*PEPCK2 decarboxylating activity does not show any effect by these metabolites and is inhibited around 80% by glutamine (Fig. 5D).

Citrate has been previously informed as a modulator of PEPCK carboxylating activity in *A. comosus* [30] and PEPCK decarboxylating activity in *A. thaliana* [40]. In the case of *Chlre*PEPCKs, the inhibitory effect of citrate on the carboxylation reaction could

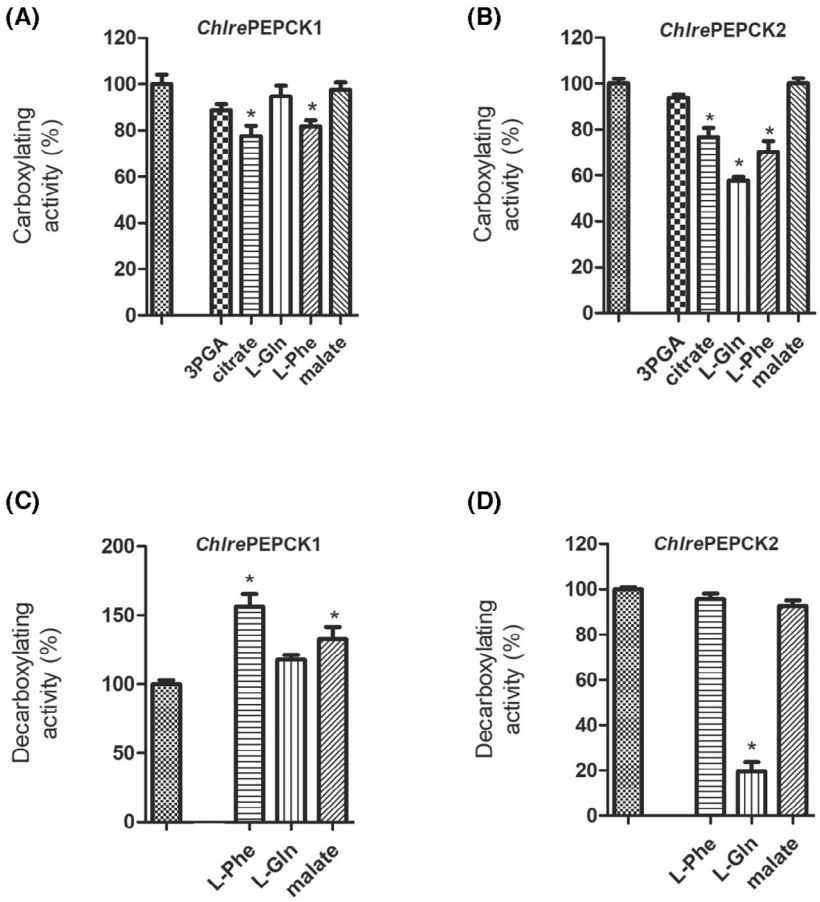

Fig. 5. Effect of metabolites on *Chlre*PEPCKs activities. Carboxylating (A, B) and decarboxylating (C, D) activities of *Chlre*PEPCK1 (A, C) and *Chlre*PEPCK2 (B, D) were measured at 2 mM of the metabolites indicated in the figure. The asterisk indicates a statistical difference ($P < 0.05$) determined using one-way ANOVA and Tukey's multiple comparison test. Data are the mean of three independent data sets ± SEM.

contribute to maintain a low PEPCK carboxylating activity to ensure gluconeogenesis (PEPCK decarboxylating activity) when acetil-CoA is available (because of acetate presence in growth medium or under lipids degradation condition). In the presence of malate, the decarboxylating activity of *Chlre*PEPCK1 is activated, stimulating the gluconeogenesis. Malate has also been described as an activator of *Ath*PEPCKs in the decarboxylation direction [40].

The modulation of *Chlre*PEPCKs activity by glutamine and phenylalanine would be another link between PEPCK and nitrogen metabolism, already described in previous reports [19,20,30,39,47]. Particularly, in *Chlamydomonas* cells, it has been previously shown that PEPCK transcript is upregulated at early stage of N deprivation but downregulated at later stages of same treatment [48]. The effect observed might indicate a feedback inhibition signal that modulates the flux of carbon directed to amino acid synthesis.

Oligomerisation analysis of *ChlrePEPCKs*

The differences in the decarboxylating parameters and response to some metabolites of the *Chlre*PEPCKs raise the possibility of a different quaternary structure between them. To further explore this point, both proteins were subjected to size exclusion Superdex 200 column (Fig. 6). At a first look, it seems that *Chlre*PEPCK1 eluted from the column as two peaks, the first one with an elution volume of 11.2 mL and the second of 14.4 mL, while *Chlre*PEPCK2 eluted as only one peak. However, a deeper analysis reveals a small peak, corresponding to an elution volume of 11.3 mL, in the *Chlre*PEPCK2 chromatogram. Furthermore, in an elution volume of approximately 13 mL, it can be seen a small peak in the *Chlre*-PEPCK1 chromatogram and a shoulder for the *Chlre*-PEPCK2. This result reflects dynamic association/disassociation equilibrium intrinsic to PEPCK in which the first 55 residues of *Chlre*PEPCK1 seem to play a fundamental role for oligomerisation. While *Chlre*-PEPCK1 behaves mainly as a hexamer of 439 kDa (peak at 11.2 mL), *Chlre*PEPCK2 behaves as a monomer (82.6 kDa). It is worth mentioning that this 14.21 mL peak of *Chlre*PEPCK2 proved to have PEPCK activity.

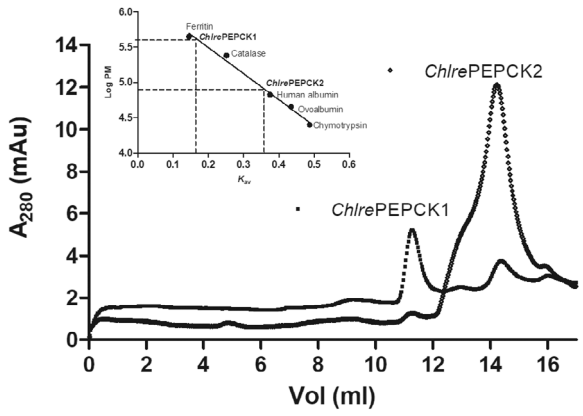

Fig. 6. Determination of the apparent molecular mass of PEPCKs proteins by size exclusion chromatography (SEC). The elution pattern of *Chlre*PEPCK1 and *Chlre*PEPCK2 are shown. Inset: Plot of partition coefficient as function of the logarithm of molecular mass, fitted with a linear function where the adjusted *R*-square was 0.998.

In the crystal dimeric structure of *T. cruzi* PEPCK (*Tc*PEPCK) [49], the authors observed that only the N-terminal domain residues from the two monomers participate in the noncovalent interactions that maintain together the dimer and identified the residues involved: $L_{10}SPE_{13}$, V_{15}, Q_{16}, L_{19}, $S_{25}RLTARG_{31}$, F_{279} and $K_{290}RTG_{293}$. According to the alignment performed with the amino acidic sequences of *Chlre*-PEPCK1 and *Tc*PEPCK (Fig. 1), the alleged residues involved in the interactions are after the first 55 residues of *Chlre*PEPCK1 ($T_{78}TPQ_{81}$), so they are present in both *Chlre*PEPCKs. Apparently, other interactions which have not been described for *Tc*PEPCK and in which these 55 N-terminal residues of *Chlre*PEPCK1 may participate, stabilises the hexameric form of the alga protein. A model of the monomeric*Chlre*PEPCK1 was built using ALPHAFOLD2 [50] but the 55 N-terminal residues could not be ordered. Also the hexameric protein cannot be modelled with ALPHAFOLD2.

Both quaternary structures found, hexameric or monomeric, were previously described for ATP-dependent PEPCK. Hexameric PEPCK was reported for PEPCK enzymes from *A. thaliana*, *U. panicoides*, *C. gayana* and *P. maximum* [34,40,46]. On the contrary, *Ec*PEPCK is representative of monomeric ATP-dependent PEPCK [51] and is also subjected to allosteric regulation [52].

Conclusions

As far as we know, this is the first biochemical report describing a PEPCK enzyme from a green alga. It seems that two PEPCK isoforms of 68 and 62 kDa could coexist in crude extracts of *C. reinhardtii*. Even though the biochemical basis for the existence of these two isoforms and their significance *in vivo* are not yet known, we could demonstrate the functionality of both enzymes *in vitro*. The higher apparent affinity for OAA and ATP than PEP and ADP and the higher

V_{max} for the decarboxylating reactions are in agreement with the general assumption that *Chlre*PEPCK primarily operates in the gluconeogenic pathway *in vivo*.

The different oligomeric state and susceptibility of *Chlre*PEPCKs activity to some metabolites *in vitro* could account for the fine control needed *in vivo* for an enzyme involved in numerous metabolic pathways. *Chlre*PEPCK2 might be originated as consequence of proteolytic regulation or alternative splicing being part of a mechanism to regulate PEPCK oligomerisation, localisation and/or activity during the adaptation to changing environmental conditions.

It has been previously described that green lineage PEPCK enzyme is subjected to regulation by allosterism, proteolysis [53] and post-translational modification (phosphorylation) [36–38]. This work suggests protein oligomerisation as an additional PEPCK control mechanism and contributes to a better understanding of the PEPCK.

Acknowledgements

This work was supported by grants from Agencia Nacional de Promoción Científica y Tecnológica (ANPCyT, PICT 2019-1771) and Universidad Nacional de Rosario (80020180300092UR). FT is a Doctoral fellow from CONICET. DFG-C, FMR and MM are research members from CONICET.

Author contributions

FT performed experiments; analyzed data; wrote the paper. FMR performed experiments; analyzed data. DGC wrote the paper; contributed reagents or other essential material. MM planned experiments; performed experiments; analyzed data; wrote the manuscript; contributed reagents or other essential material.

Data accessibility

The data that support the findings of this study are available in Figs 1–6.

References

1 Utter MF and Kolenbrander HM (1972) Formation of oxalacetate by CO_2 fixation on phosphoenolpyruvate. In The Enzymes (Boyer PD, ed.), pp. 117–168. Elsevier, Amsterdam.
2 Leegood RC and Walker RP (2003) Regulation and roles of phosphoenolpyruvate carboxykinase in plants. *Arch Biochem Biophys* **414**, 204–210.
3 Rosewich UL and Kistler HC (2000) Role of horizontal gene transfer in the evolution of fungi. *Annu Rev Phytopathol* **38**, 325–363.
4 Chiba Y, Miyakawa T, Shimane Y, Takai K, Tanokura M and Nozaki T (2019) Structural comparisons of phosphoenolpyruvate carboxykinases reveal the evolutionary trajectories of these phosphodiester energy conversion enzymes. *J Biol Chem* **294**, 19269–19278.
5 Koendjbiharie JG, van Kranenburg R and Kengen SW (2021) The PEP-pyruvate-oxaloacetate node: variation at the heart of metabolism. *FEMS Microbiol Rev* **45**, fuaa061.
6 Leegood R and Ap Rees T (1978) Phosphoenolpyruvate carboxykinase and gluconeogenesis in cotyledons of *Cucurbita pepo*. *Biochim Biophys Acta* **524**, 207–218.
7 Trevanion SJ, Brooks AL and Leegood RC (1995) Control of gluconeogenesis by phosphoenolpyruvate carboxykinase in cotyledons of *Cucurbita pepo* L. *Planta* **196**, 653–658.
8 Martín M, Plaxton WC and Podestá FE (2007) Activity and concentration of non-proteolyzed phosphoenolpyruvate carboxykinase in the endosperm of germinating castor oil seeds: effects of anoxia on its activity. *Physiol Plant* **130**, 484–494.
9 Eastmond PJ and Graham IA (2001) Re-examining the role of the glyoxylate cycle in oilseeds. *Trends Plant Sci* **6**, 72–78.
10 Penfield S, Rylott EL, Gilday AD, Graham S, Larson TR and Graham IA (2004) Reserve mobilization in the Arabidopsis endosperm fuels hypocotyl elongation in the dark, is independent of abscisic acid, and requires PHOSPHOENOLPYRUVATE CARBOXYKINASE1. *Plant Cell* **16**, 2705–2718.
11 Eastmond PJ, Astley HM, Parsley K, Aubry S, Williams BP, Menard GN, Craddock CP, Nunes-Nesi A, Fernie AR and Hibberd JM (2015) Arabidopsis uses two gluconeogenic gateways for organic acids to fuel seedling establishment. *Nat Commun* **6**, 1–8.
12 Reiskind JB and Bowes G (1991) The role of phosphoenolpyruvate carboxykinase in a marine macroalga with C4-like photosynthetic characteristics. *Proc Natl Acad Sci USA* **88**, 2883–2887.
13 Morel FM, Cox EH, Kraepiel AM, Lane TW, Milligan AJ, Schaperdoth I, Reinfelder JR and Tortell PD (2002) Acquisition of inorganic carbon by the marine diatom *Thalassiosira weissflogii*. *Funct Plant Biol* **29**, 301–308.
14 Reinfelder JR, Kraepiel AM and Morel FM (2000) Unicellular C 4 photosynthesis in a marine diatom. *Nature* **407**, 996–999.
15 Reinfelder JR, Milligan AJ and Morel FM (2004) The role of the C4 pathway in carbon accumulation and fixation in a marine diatom. *Plant Physiol* **135**, 2106–2111.

16 McGinn PJ and Morel FM (2008) Expression and regulation of carbonic anhydrases in the marine diatom *Thalassiosira pseudonana* and in natural phytoplankton assemblages from Great Bay, New Jersey. *Physiol Plant* **133**, 78–91.
17 Dittrich P, Campbell WH and Black C (1973) Phosphoenolpyruvate carboxykinase in plants exhibiting crassulacean acid metabolism. *Plant Physiol* **52**, 357–361.
18 Edwards G, Kanai R and Black C (1971) Phosphoenolpyruvate carboxykinase in leaves of certain plants which fix CO2 by the C4-dicarboxylic acid cycle of photosynthesis. *Biochem Biophys Res Commun* **45**, 278–285.
19 Walker RP, Chen Z-H, Técsi LI, Famiani F, Lea PJ and Leegood RC (1999) Phosphoenolpyruvate carboxykinase plays a role in interactions of carbon and nitrogen metabolism during grape seed development. *Planta* **210**, 9–18.
20 Lea P, Chen Z-H, Leegood R and Walker R (2001) Does phosphoenolpyruvate carboxykinase have a role in both amino acid and carbohydrate metabolism? *Amino Acids* **20**, 225–241.
21 Goodstein DM, Shu S, Howson R, Neupane R, Hayes RD, Fazo J, Mitros T, Dirks W, Hellsten U and Putnam N (2012) Phytozome: a comparative platform for green plant genomics. *Nucleic Acids Res* **40**, D1178–D1186.
22 Tardif M, Atteia A, Specht M, Cogne G, Rolland N, Brugière S, Hippler M, Ferro M, Bruley C and Peltier G (2012) PredAlgo: a new subcellular localization prediction tool dedicated to green algae. *Mol Biol Evol* **29**, 3625–3639.
23 Thompson JD, Higgins DG and Gibson TJ (1994) CLUSTAL W: improving the sensitivity of progressive multiple sequence alignment through sequence weighting, position-specific gap penalties and weight matrix choice. *Nucleic Acids Res* **22**, 4673–4680.
24 Harris EH (1989) Chlamydomonas Sourcebook. Academic Press, San Diego, CA.
25 Pfaffl MW (2001) A new mathematical model for relative quantification in real-time RT–PCR. *Nucleic Acids Res* **29**, e45.
26 Carrillo JB, Gomez-Casati DF, Martín M and Busi MV (2018) Identification and analysis of OsttaDSP, a phosphoglucan phosphatase from *Ostreococcus tauri*. *PLoS ONE* **13**, e0191621.
27 Carrillo JB, Torresi F, Morales LL, Ricordi M, Gomez-Casati DF, Busi MV and Martín M (2020) Identification and characterization of ChlreSEX4, a novel glucan phosphatase from *Chlamydomonas reinhardtii* green alga. *Arch Biochem Biophys* **680**, 108235.
28 Wu F-S and Wang M-Y (1984) Extraction of proteins for sodium dodecyl sulfate-polyacrylamide gel electrophoresis from protease-rich plant tissues. *Anal Biochem* **139**, 100–103.
29 Méchin V, Damerval C and Zivy M (2007) Total protein extraction with TCA-acetone. In Plant Proteomics (Thiellement H, Zivy M, Damerval C and Méchin V, eds), pp. 1–8. Springer, Berlin.
30 Martín M, Rius SP and Podestá FE (2011) Two phosphoenolpyruvate carboxykinases coexist in the Crassulacean acid metabolism plant *Ananas comosus*. Isolation and characterization of the smaller 65 kDa form. *Plant Physiol Biochem* **49**, 646–653.
31 Plaxton WC (1989) Molecular and immunological characterization of plastid and cytosolic pyruvate kinase isozymes from castor-oil-plant endosperm and leaf. *Eur J Biochem* **181**, 443–451.
32 Matte A, Goldie H, Sweet RM and Delbaere LT (1996) Crystal structure of *Escherichia coli* Phosphoenolpyruvate Carboxykinase: a new structural family with the P-loop nucleoside triphosphate hydrolase fold. *J Mol Biol* **256**, 126–143.
33 Traut TW (1994) The functions and consensus motifs of nine types of peptide segments that form different types of nucleotide-binding sites. *EJB Rev* **1994**, 105–115.
34 Finnegan PM and Burnell JN (1995) Isolation and sequence analysis of cDNAs encoding phosphoenolpyruvate carboxykinase from the PCK-type C 4 grass *Urochloa panicoides*. *Plant Mol Biol* **27**, 365–376.
35 Kim D-J and Smith SM (1994) Molecular cloning of cucumber phosphoenolpyruvate carboxykinase and developmental regulation of gene expression. *Plant Mol Biol* **26**, 423–434.
36 Chao Q, Liu X-Y, Mei Y-C, Gao Z-F, Chen Y-B, Qian C-R, Hao Y-B and Wang B-C (2014) Light-regulated phosphorylation of maize phosphoenolpyruvate carboxykinase plays a vital role in its activity. *Plant Mol Biol* **85**, 95–105.
37 Walker RP and Leegood RC (1995) Purification, and phosphorylation in vivo and in vitro, of phosphoenolpyruvate carboxykinase from cucumber cotyledons. *FEBS Lett* **362**, 70–74.
38 Walker RP and Leegood RC (1996) Phosphorylation of phosphoenolpyruvate carboxykinase in plants. Studies in plants with C4 photosynthesis and Crassulacean acid metabolism and in germinating seeds. *Biochem J* **317**, 653–658.
39 Walker RP, Chen Z-H and Famiani F (2021) Gluconeogenesis in plants: a key Interface between organic acid/amino acid/lipid and sugar metabolism. *Molecules* **26**, 5129.
40 Rojas BE, Hartman MD, Figueroa CM, Leaden L, Podestá FE and Iglesias AA (2019) Biochemical characterization of phospho enol pyruvate carboxykinases from *Arabidopsis thaliana*. *Biochem J* **476**, 2939–2952.

41 Tsiatsiani L, Timmerman E, De Bock P-J, Vercammen D, Stael S, Van De Cotte B, Staes A, Goethals M, Beunens T and Van Damme P (2013) The Arabidopsis metacaspase9 degradome. *Plant Cell* **25**, 2831–2847.
42 Merchant SS, Prochnik SE, Vallon O, Harris EH, Karpowicz SJ, Witman GB, Terry A, Salamov A, Fritz-Laylin LK and Maréchal-Drouard L (2007) The Chlamydomonas genome reveals the evolution of key animal and plant functions. *Science* **318**, 245–250.
43 Pandey M, Stormo GD and Dutcher SK (2020) Alternative splicing during the *Chlamydomonas reinhardtii* cell cycle. *G3 (Bethesda)* **10**, 3797–3810.
44 Walker RP, Trevanion SJ and Leegood RC (1995) Phosphoenolpyruvate carboxykinase from higher plants: purification from cucumber and evidence of rapid proteolytic cleavage in extracts from a range of plant tissues. *Planta* **196**, 58–63.
45 Walker RP, Chen Z-H, Acheson RM and Leegood RC (2002) Effects of phosphorylation on phosphoenolpyruvate carboxykinase from the C4 plant Guinea grass. *Plant Physiol* **128**, 165–172.
46 Burnell J (1986) Purification and properties of phosphoenolpyruvate carboxykinase from C4 plants. *Funct Plant Biol* **13**, 577–587.
47 Wingler A, Walker RP, Chen Z-H and Leegood RC (1999) Phosphoenolpyruvate carboxykinase is involved in the decarboxylation of aspartate in the bundle sheath of maize. *Plant Physiol* **120**, 539–546.
48 Park JJ, Wang H, Gargouri M, Deshpande RR, Skepper JN, Holguin FO, Juergens MT, Shachar-Hill Y, Hicks LM and Gang DR (2015) The response of *Chlamydomonas reinhardtii* to nitrogen deprivation: a systems biology analysis. *Plant J* **81**, 611–624.
49 Trapani S, Linss J, Goldenberg S, Fischer H, Craievich AF and Oliva G (2001) Crystal structure of the dimeric phosphoenolpyruvate carboxykinase (PEPCK) from *Trypanosoma cruzi* at 2 Å resolution. *J Mol Biol* **313**, 1059–1072.
50 Mirdita M, Schütze K, Moriwaki Y, Heo L, Ovchinnikov S and Steinegger M (2022) ColabFold: making protein folding accessible to all. *Nat Methods* **19**, 679–682.
51 Tari LW, Matte A, Goldie H and Delbaere LT (1997) Mg(2+)–Mn2+ clusters in enzyme-catalyzed phosphoryl-transfer reactions. *Nat Struct Biol* **4**, 990–994.
52 Goldie A and Sanwal BD (1980) Allosteric control by calcium and mechanism of desensitization of phosphoenolpyruvate carboxykinase of *Escherichia coli*. *J Biol Chem* **255**, 1399–1405.
53 Rojas BE, Hartman MD, Figueroa CM and Iglesias AA (2021) Proteolytic cleavage of *Arabidopsis thaliana* phospho enol pyruvate carboxykinase-1 modifies its allosteric regulation. *J Exp Bot* **72**, 2514–2524.